Electrochemistry Communications 69 (2016) 41–45

Contents lists available at ScienceDirect

Electrochemistry Communications

journal homepage: www.elsevier.com/locate/elecom

pH-induced reversal of ionic diode polarity in 300 nm thin membranes based on a polymer of intrinsic microporosity

Yuanyang Rong [a], Qilei Song [b], Klaus Mathwig [c], Elena Madrid [a], Daping He [a], Ralf G. Niemann [a], Petra J. Cameron [a], Sara E.C. Dale [d], Simon Bending [d], Mariolino Carta [e], Richard Malpass-Evans [e], Neil B. McKeown [e], Frank Marken [a,*]

[a] Department of Chemistry, University of Bath, Claverton Down, Bath BA2 7AY, UK
[b] Department of Chemical Engineering, Imperial College London, London SW7 2AZ, UK
[c] Pharmaceutical Analysis, Groningen Research Institute of Pharmacy, University of Groningen, P.O. Box 196, 9700 AD Groningen, The Netherlands
[d] Department of Physics, University of Bath, Claverton Down, Bath BA2 7AY, UK
[e] School of Chemistry, University of Edinburgh, David Brewster Road, Edinburgh EH9 3FJ, UK

ARTICLE INFO

Article history:
Received 2 May 2016
Received in revised form 13 May 2016
Accepted 24 May 2016
Available online 27 May 2016

Keywords:
Electrokinetic effects
Salt separation
Membrane potential
Nanofluidics
Iontronics
Electrophysiology

ABSTRACT

"Ionic diode" (or current rectification) effects are potentially important for a range of applications including water purification. In this preliminary report, we observe novel ionic diode behaviour of thin (300 nm) membranes based on a polymer of intrinsic microporosity (PIM-EA-TB) supported on a poly-ethylene-terephthalate (PET) film with a 20 μm diameter microhole, and immersed in aqueous electrolyte media. Current rectification effects are observed for half-cells with the same electrolyte solution on both sides of the membrane for cases where cation and anion mobility differ (HCl, other acids, NaOH, etc.) but not for cases where cation and anion mobility are more alike (LiCl, NaCl, KCl, etc.). A pH-dependent reversal of the ionic diode effect is observed and discussed in terms of tentatively assigned mechanisms based on both (i) ion mobility within the PIM-EA-TB nano-membrane and (ii) a possible "mechanical valve effect" linked to membrane potential and electrokinetic movement of the membrane as well as hydrostatic pressure effects.

1. Introduction

Interest in "ionic devices" [1–5] has increased over the recent years with the emergence of new nanopore technologies [6,7] and availability of new microporous materials [8]. The potential for applications of these devices ranges from analytical nanofluidic tools [9], natural cell pore mimics [10], to energy harvesting systems, and ionic rectifiers for desalination [11]. Ionic rectification (or "ionic diode" [12]) effects are well-known in particular for gel-junctions [13] and hydrogel materials [14]. Both nano-engineered nano-pores and novel microporous materials can contribute to the development of ionic rectifiers and devices. There are opportunities to exploit properties of new types of microporous materials (such as polymers of intrinsic microporosity or PIMs) for improved ionic diodes. In this preliminary report we explore the effects on ion flow by applying very thin PIM membranes produced by spin-coating followed by lift off and transfer.

Polymers of intrinsic microporosity [15,16] have emerged recently as a novel class of materials based on molecularly highly rigid structures that are highly processable (e.g. soluble in organic solvents for casting of films and membranes [17]) and highly porous with typical BET surface area values $\approx 1000\ m^2\ g^{-1}$ [18]. Initial work focused on the gas-phase, but recently also liquid-phase applications have been explored based on stabilisation of fuel cell catalysts [19], "heterogenisation" of molecular catalysts [20,21], formation of novel microporous heterocarbon structures [22], and current rectification [23]. In previous work we employed solution casting methods to give relatively thick (typically 10 μm or more) PIM membranes. However, it is highly interesting to explore much thinner polymer nano-membranes. It is demonstrated here, that even very thin films of PIM-EA-TB (with typically 300 nm thickness) can be employed successfully for current rectification in ionic diode devices.

2. Experimental

2.1. Chemical reagents

Polymer PIM-EA-TB was prepared following a literature procedure [18]. Hydrochloric acid (37%), perchloric acid (70%), sulphuric acid (98%) and phosphoric acid (85%), and electrolyte salts were obtained

* Corresponding author.
E-mail address: f.marken@bath.ca.uk (F. Marken).

http://dx.doi.org/10.1016/j.elecom.2016.05.019
1388-2481/

from Sigma-Aldrich or Fisher Scientific and used without further purification. Solutions were prepared with deionised water of resistivity 18.2 MΩ cm (at 20 °C) from a Thermo Scientific water purification system.

2.2. Instrumentation

A potentiostat system (Ivium Compactstat) was employed with Pt wires as working/counter electrodes, and two KCl-saturated calomel reference electrodes (SCE, Radiometer, Copenhagen) as sense and reference electrode in a 4-electrode membrane cell (Fig. 1A). The membrane sample was always on the side of the working electrode.

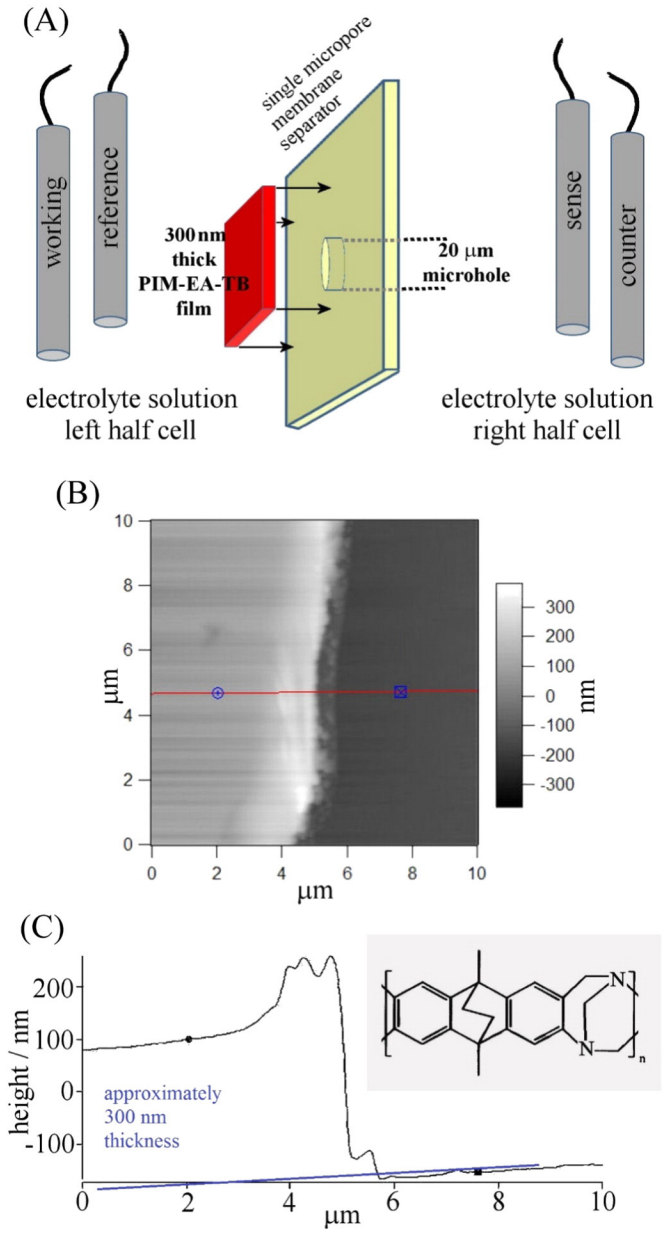

Fig. 1. (A) Schematic drawing of the 4-electrode membrane polarisation experiment based on a 20 μm diameter microhole that is covered with a typically 300 nm thin PIM-EA-TB membrane. (B) AFM image of the spin-coated PIM-EA-TB membrane after cutting to reveal the thickness. (C) Cross-sectional profile (inset molecular structure of PIM-EA-TB).

2.3. Preparation of nano-membranes

A thin PIM-EA-TB film was spin-coated on a cover glass using 2 wt.% PIM-EA-TB in chloroform solution (Laurell WS-650Mz-23NPP, 2000 rpm for 1 min). Next, the PIM-EA-TB film was lifted off in water and then transferred to a PET film with a ca. 20 μm diameter microhole (supplied by Laser Micromachining Limited, St. Asaph, Denbighshire LL17 0JG, UK). AFM thickness measurements of the PIM-EA-TB film on a glass slide in dry ambient conditions (Fig. 1B, C) reveal typically 300 nm thickness produced with this concentration of PIM-EA-TB.

3. Results and discussion

3.1. Electrolyte and pH effects

Fig. 2A shows cyclic voltammetry data for a 300 nm thin PIM-EA-TB film covering a 20 μm diameter microhole in a 6 μm thick PET film. The data for 10 mM HCl (Fig. 2Ai) clearly show very low currents in the positive potential range ("closed" diode) and significant currents in the negative potential range ("open" diode). Schematic diagrams in Fig. 2E and F tentatively (following a mechanism suggested in earlier work [11]) explain this behaviour at least qualitatively based on protonation of the amine sites in PIM-EA-TB (see structure in Fig. 1) leading to mixed proton and chloride conductivity. In the "open" diode state, the depletion effect may occur at the open side exposed to the electrolyte solution. In contrast, in the "closed" diode state depletion occurs in a restricted region and therefore causes a significant drop in current and the rectification effect. When extracting currents at −1 V and +1 V, the rectification ratio for the "nano-membrane" (defined here as I_{open}/I_{closed}) is 180 (compared to 576 reported recently for data obtained for much thicker PIM-EA-TB deposits [23]).

Additional chronoamperometry experiments were conducted switching the applied potential between +1 V and −1 V (see Fig. 2B) and it can be observed that the current switches rapidly from +0.03 μA to −5.0 μA consistent with a rectification ratio of 180. Similar experiments performed with 10 mM NaCl do not result in significant rectification effects although conductivity through the membrane is observed (see Fig. 2Aii). That is, both Na^+ and Cl^- are likely to move through the porous PIM-EA-TB structure, but ion mobilities are similar and significant depletion effects do not arise. Interestingly, for the case of 10 mM NaOH, there is again a current rectification effect (see Fig. 2Aiii). Chronoamperometry data in Fig. 2Bii show that, when switching the potential from −1 V to +1 V, the current switches from −0.02 μA to 1.6 μA, suggesting a difference in mobility for Na^+ and OH^- in PIM-EA-TB causing a reversal of the ionic diode polarity. Data in Fig. 2C and D show the gradual change in rectification effects with pH consistent with an approximate pK_A for PIM-EA-TB at pH 4 [23].

3.2. Ionic strength effects

When changing the concentration for HCl and for NaOH, currents increase but the rectification ratio at +1 V and −1 V remains approximately constant (Fig. 3A–B). However, when surveying different types of acids, a clear trend is observed with HCl giving good rectification effects followed by $HClO_4$, H_2SO_4, and H_3PO_4 giving only poor rectification effects with rectification ratios of 180, 51, 8.0, and 6.7, respectively (Fig. 3C). The poorer rectification effects with H_3PO_4 are likely to be linked to phosphoric acid exhibiting pK_A values higher than that of the PIM-EA-TB, and therefore providing additional protons to weaken the ion depletion effect. When comparing neutral electrolyte media for a range of different anions (see Fig. 3D), significant rectification effects are observed also for BF_4^-, suggesting that the nature of the anion also

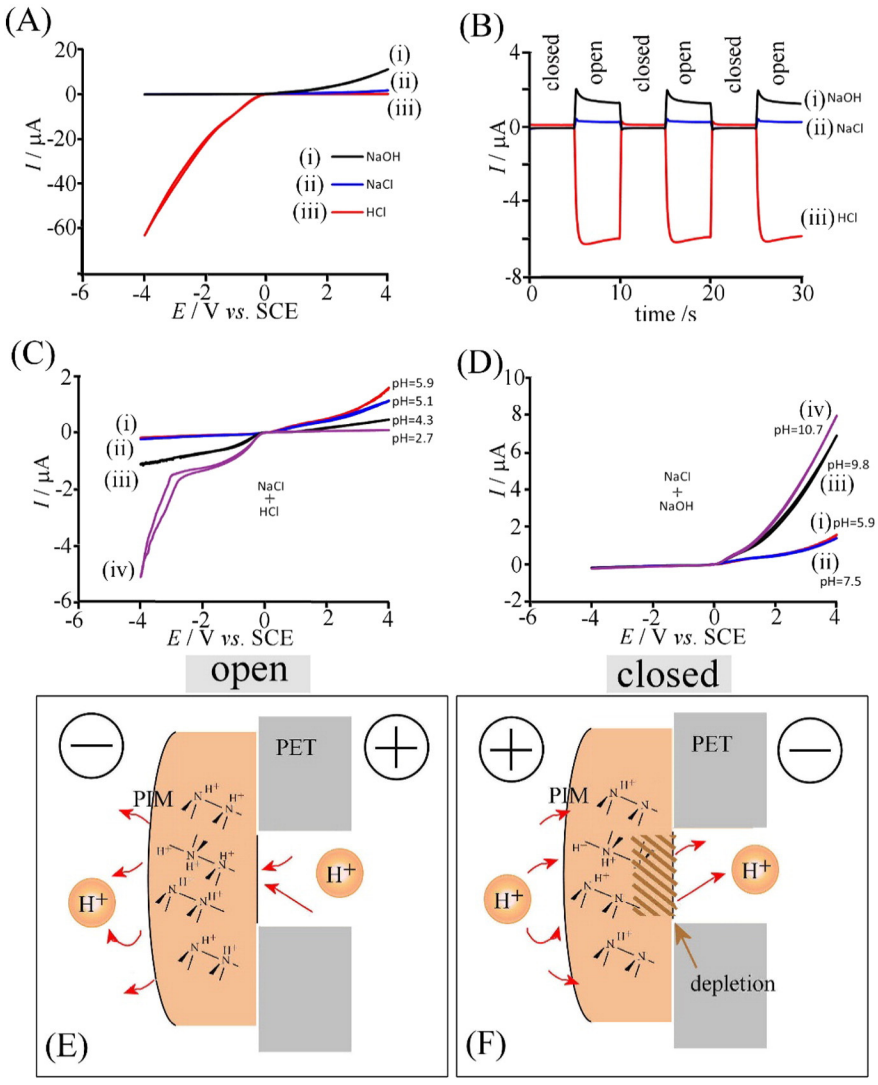

Fig. 2. (A) Cyclic voltammograms (50 mV s^{-1}) for a PIM-EA-TB membrane in 10 mM HCl, 10 mM NaCl, and 10 mM NaOH. (B) Chronoamperometry (+1 and −1 V) for 10 mM HCl, 10 mM NaCl, and 10 mM NaOH. (C) Cyclic voltammograms (50 mV s^{-1}) for 10 mM NaCl with the pH adjusted with HCl. (D) As before, but with the pH adjusted with NaOH. (E, F) Schematic drawing of the ionic diode in "open" and "closed" states.

can have a strong effect on current rectification phenomena in the PIM-EA-TB membrane.

3.3. Hydrostatic pressure effects

Measurements were performed for 10 mM HCl (Fig. 3E) and for 10 mM NaOH (Fig. 3F) by varying the hydrostatic pressure across the measurement cell by simply adding or removing electrolyte solution (see inset in Fig. 3F, data for 0, ±5, and ±10 cm water column). For HCl the ionic diode effect is significantly affected by hydrostatic pressure, whereas the effects for NaOH are small. Strikingly, the "open diode" current is increased when additional pressure is applied. This suggests that further "opening" or "tuning" of the diode could be linked to a "mechanical valve" phenomenon, where "bulging" of the thin PIM-EA-TB nanomembrane over the 20 µm microhole will cause a geometry change and thereby contribute to additional changes in flow of current. Further work, for example revealing how membrane potential (associated with electrokinetic effects) and ion size effects are linked to the observed phenomena, will be necessary to identify, quantify, and exploit the processes behind these PIM nano-membrane-based current rectification effects.

4. Conclusion

It has been shown that a very thin (300 nm) PIM-EA-TB membrane can generate significant "ionic diode" effects and could therefore be employed in ionic rectifier-based devices. The switch in ionic diode polarity is novel and linked to the pH of the electrolyte. This phenomenon is explained here tentatively as based on (i) ion mobility differences within the PIM-EA-TB film and (ii) a valve-like opening of the membrane (driven by electrokinetic or hydrostatic effects) over the supporting PET film microhole. Further work will be required, experimentally and theoretically, to better understand ion mobility and reactivity within PIM films and to further develop and exploit these phenomena in areas such as energy harvesting and desalination.

Acknowledgements

Y.R. thanks the University of Bath for a fee waiver and the China Scholarship Council for a PhD stipend. E.M. acknowledges financial support from the EPSRC (EP/K004956/1). F.M. and N.B.M. gratefully acknowledge the Leverhulme Trust for support (RPG-2014-308).

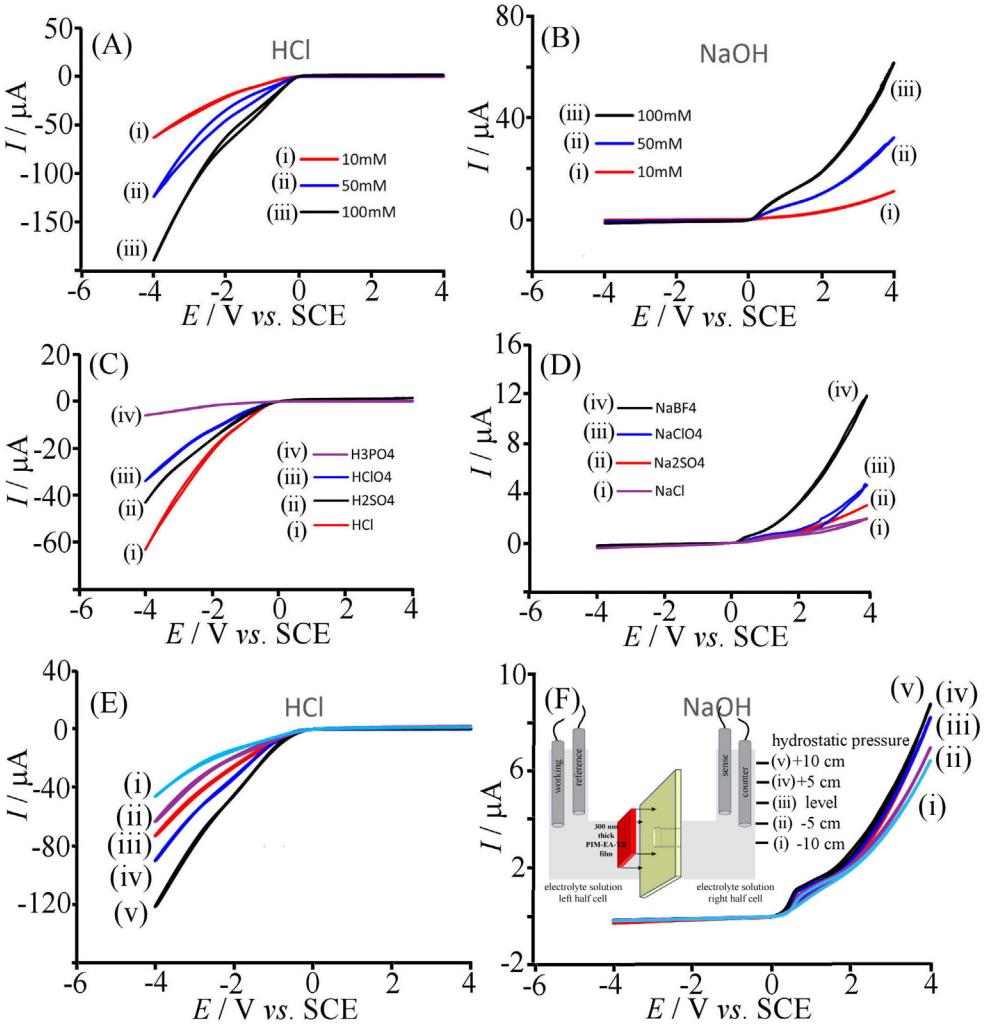

Fig. 3. (A) Cyclic voltammograms (50 mV s^{-1}) for PIM-EA-TB membrane in (i) 10 mM, (ii) 50 mM, and (iii) 100 mM HCl. (B) As above, but for (i) 10 mM NaOH, (ii) 50 mM NaOH, and (iii) 100 mM NaOH. (C) Cyclic voltammograms (50 mV s^{-1}) for a PIM-EA-TB membrane in 10 mM HCl (i), H_2SO_4 (ii), $HClO_4$ (iii), and H_3PO_4 (iv). (D) As above, but with 10 mM Na_2SO_4 (i), NaCl (ii), $NaClO_4$ (iii), and $NaBF_4$ (iv). (E) Cyclic voltammograms (50 mV s^{-1}) for a PIM-EA-TB membrane in 10 mM HCl with varying hydrostatic pressure (see F inset, the fill-height of one half-cell relative to the second was systematically varied by adding or removing electrolyte to give (i) −10, (ii) −5, (iii) 0, (iv) +5, and (v) +10 cm hydrostatic pressure in the counter relative to the working compartment). (F) As before, but for 10 mM NaOH.

References

[1] H. Chun, T.D. Chung, Iontronics, Annu. Rev. Anal. Chem. 8 (2015) 441–462.
[2] L. Hegedus, N. Kirschner, M. Wittmann, Z. Noszticzius, Electrolyte transistors: ionic reaction–diffusion systems with amplifying properties, J. Phys. Chem. A 102 (1998) 6491–6497.
[3] G.C. Sun, S.Y. Senapati, H.C. Chang, High-flux ionic diodes, ionic transistors and ionic amplifiers based on external ion concentration polarization by an ion exchange membrane: a new scalable ionic circuit platform, Lab Chip 16 (2016) 1171–1177.
[4] R. Zhao, G.H. He, Y.L. Deng, Non-water ionic diode based on bias-dependent precipitation, Electrochem. Commun. 23 (2012) 106–109.
[5] E. Madrid, Y.Y. Rong, M. Carta, N.B. McKeown, R. Malpass-Evans, G.A. Attard, T.J. Clarke, S.H. Taylor, Y.T. Long, F. Marken, Metastable ionic diodes derived from an amine-based polymer of intrinsic microporosity, Angew. Chem. Int. Ed. 53 (2014) 10751–10754.
[6] J.K. Rosenstein, S.G. Lemay, K.L. Shepard, Nanopores single-molecule bioelectronics, WIREs Nanomed. Nanobiotechnol. 7 (2015) 475–493.
[7] Z.S. Siwy, S. Howorka, Engineered voltage-responsive Nanopores, Chem. Soc. Rev. 39 (2010) 1115–1132.
[8] E. Madrid, M.A. Buckingham, J.M. Stone, A.T. Rogers, W.J. Gee, A.D. Burrows, P.R. Raithby, V. Celorrio, D.J. Fermin, F. Marken, Ion flow in a zeolitic imidazolate framework results in ionic diode phenomena, Chem. Commun. 52 (2016) 2792–2794.
[9] A. Gencoglu, A.R. Minerick, Electrochemical detection techniques in micro- and nanofluidic devices, Microfluid. Nanofluid. 17 (2014) 781–807.
[10] N.N. Liu, Z.K. Yang, X.W. Ou, B.M. Wei, J.T. Zhang, Y.M. Jia, F. Xia, Nanopore-based analysis of biochemical species, Microchim. Acta 183 (2016) 955–963.
[11] E. Madrid, P. Cottis, Y.Y. Rong, A.T. Rogers, J.M. Stone, R. Malpass-Evans, M. Carta, N.B. McKeown, F. Marken, Water desalination concept using an ionic rectifier based on a polymer of intrinsic microporosity (PIM), J. Mater. Chem. A3 (2015) 15849–15853.
[12] W. Guo, Y. Tian, L. Jiang, Asymmetric ion transport through ion-channel-mimetic solid-state nanopores, Acc. Chem. Res. 46 (2013) 2834–2846.
[13] B. Lovrecek, A. Despic, J.O.M. Bockris, Electrolytic junctions with rectifying properties, J. Phys. Chem. 63 (1959) 750–751.
[14] H.J. Koo, O.D. Velev, Ionic current devices-recent progress in the merging of electronic, microfluidic, and biomimetic structures, Biomicrofluidics 7 (2013) 031501.
[15] N.B. McKeown, P.M. Budd, Exploitation of intrinsic microporosity in polymer-based materials, Macromolecules 43 (2010) 5163–5176.
[16] P.M. Budd, B.S. Ghanem, S. Makhseed, N.B. McKeown, K.J. Msayib, C.E. Tattershall, Polymers of intrinsic microporosity (PIMs): robust, solution-processable, organic nanoporous materials, Chem. Commun. (2004) 230–231.
[17] F.J. Xia, M. Pan, S.C. Mu, R. Malpass-Evans, M. Carta, N.B. McKeown, G.A. Attard, A. Brew, D.J. Morgan, F. Marken, Polymers of intrinsic microporosity in electrocatalysis: novel pore rigidity effects and lamella palladium growth, Electrochim. Acta 128 (2014) 3–9.
[18] M. Carta, R. Malpass-Evans, M. Croad, Y. Rogan, J.C. Jansen, P. Bernardo, F. Bazzarelli, N.B. McKeown, An efficient polymer molecular sieve for membrane gas separations, Science 339 (2013) 303–307.
[19] D.P. He, Y.Y. Rong, Z.K. Kou, S.C. Mu, T. Peng, R. Malpass-Evans, M. Carta, N.B. McKeown, F. Marken, Intrinsically microporous polymer slows down fuel cell catalyst corrosion, Electrochem. Commun. 59 (2015) 72–76.
[20] Y.Y. Rong, R. Malpass-Evans, M. Carta, N.B. McKeown, G.A. Attard, F. Marken, High density heterogenisation of molecular electrocatalysts in a rigid intrinsically microporous polymer, Electrochem. Commun. 46 (2014) 26–29.
[21] S.D. Ahn, A. Kolodziej, R. Malpass-Evans, M. Carta, N.B. McKeown, S.D. Bull, A. Buchard, F. Marken, Polymer of intrinsic microporosity induces host–guest

substrate selectivity in heterogeneous 4-benzoyloxy-TEMPO-catalysed alcohol oxidations, Electrocatalysis 7 (2016) 70–78.
[22] Y.Y. Rong, D.P. He, A. Sanchez-Fernandez, C. Evans, K.J. Edler, R. Malpass-Evans, M. Carta, N.B. McKeown, T.J. Clarke, S.H. Taylor, F. Marken, Carbon intrinsically microporous polymer retains porosity in vacuum thermolysis to electroactive heterocarbon, Langmuir 31 (2015) 12300–12306.
[23] Y.Y. Rong, A. Kolodziej, E. Madrid, M. Carta, R. Malpass-Evans, N.B. McKeown, F. Marken, Polymers of intrinsic microporosity in electrochemistry: anion uptake and transport effects in thin film electrodes and in free-standing ionic diode membranes, J. Electroanal. Chem. (2015), http://dx.doi.org/10.1016/j.jelechem.2015.11.038.